Research Article

Designing and Simulation of Permanent Magnet Synchronous Generator for Wind Energy Hybrid System

Shoaib Khan[1], Sida Hussain[2], Amir Naveed[1*], Nazia Wali[3], Zafar Ullah[1], Muhammad Arif[1], Muhammad Sadiq[4] and Muhammad Asif[5]

[1]Center for Advanced Studies in Energy Engineering, University of Engineering and Technology, Peshawar, Khyber Pakhtunkhwa, Pakistan; [2]Department of Civil Engineering, University of Engineering and Technology, Peshawar, Khyber Pakhtunkhwa, Pakistan; [3]Faculty of Computing, Riphah International University, Islamabad, Pakistan; [4]Department of Mechanical Engineering, University of Engineering and Technology, Peshawar, Khyber Pakhtunkhwa, Pakistan; [5]Department of Electronics, University of Peshawar, Khyber Pakhtunkhwa, Pakistan.

Abstract: Renewable energy technologies are the main focus in today's world for scientists and engineers due to global climate issues. Energy extracted from wind and solar are the two most established ones as more than 5% of electricity is produced from wind globally. This paper gives insight knowledge to the energy planners for developing a cost-effective way to mitigate the electricity problems in low-income areas by incorporating the energy mix of wind and solar. A Surface Mounted Permanent Magnet Synchronous Generator is designed for the location and simulated in Matlab. With a fixed rated speed of 100 *rpm*, based on the load calculation, the number of poles and slots calculated are 60 and 180 respectively. The total load demand is shared 50% between wind and solar as per the load demand of the locality. The total capacity of the generator designed is 60*kW*. Sensitivity analysis of the designed machine is done by varying the hyper-parameters of the wind turbine generators.

Received: November 27, 2020; **Accepted:** June 19, 2021; **Published:** June 30, 2021
***Correspondence:** Amir Naveed, Center for Advanced Studies in Energy Engineering, University of Engineering and Technology, Peshawar, Khyber Pakhtunkhwa, Pakistan; **Email:** amirkhattak@uetpeshawar.edu.pk
Citation: Khan, S., S. Hussain, A. Naveed, N. Wali, Z. Ullah, M. Arif, M. Sadiq and M. Asif. 2021. Designing and simulation of permanent magnet synchronous generator for wind energy hybrid system. *Journal of Engineering and Applied Sciences,* 40(1): 52-59.
DOI: https://dx.doi.org/10.17582/journal.jeas/40.1.52.59
Keywords: Permanent magnet synchronous generator, Doubly fed induction generator, Wound rotor induction generator, Squirrel cage induction generator, Technique of order preference similarity to ideal solution

Introduction

The worldwide increasing environmental and ecological constraints resulted from the extraction of energy from fossil fuels with its limited availability in the future (Herbet *et al.*, 2007), has compelled the world policymakers on renewables to look for alternate resources of energy. Besides the depletion of fossil fuels, the environmental concerns due to the emission of CO_2 gas, which has its role in Global Warming and other toxic gases are some of the major restraints that have highlighted the energy demand from the non-conventional resources (Chiari *et al.*, 2011). Renewable energy exists in the form of solar, wind, hydro, biomass, geothermal, and tidal energy in nature (Alrikabi, 2014). If only wind energy is taken into account as this paper would deal, then it is important to understand the scientific reason behind the existence of wind on earth's atmosphere as it is only possible to get feasible energy out of the wind on earth's atmosphere where wind speed is sustainable to rotate the wind turbine. The different weather patterns resulted from the uneven terrain on the earth's surface and geographical tilt causes different heat conditions

near the surface of the earth from the sun that causes the wind to blow from higher atmospheric pressure to lower atmospheric pressure (Herbet *et al.*, 2007). According to the multi-criteria decision analysis (Saleem and Ulfat, 2019), conducted for the different alternatives for the household domestic sector in Pakistan, wind energy is ranked the second most feasible alternative for the household energy demand sector. In Permanent Magnet Synchronous Generator (PMSG) was designed for 1500W rated power (Hebala *et al.*, 2017). In this paper, the PMSG Wind turbine generator is designed for 60kW rated power and its simulation is done by using Matlab Simulink software. The structure of this paper is categorized as follows: The ratings/specifications of the generator along with the comparative analysis between different topologies of generators consisting of the Squirrel Cage Induction Generator (SCIG), Doubly Fed Induction Generator (DFIG), and Permanent Magnet Synchronous Generator (PMSG) are studied in section I. The type of generator with the highest performance is considered for the locality along with its topology. The methodology of the designed machine is explained in section II. The designed machine sensitivity is evaluated against its calculated parameters in the result and analysis section III. In the end, the conclusion has been highlighted in section IV.

Rating/specification of wind generator

The design of the Generator from the Wind Turbine is based on 100 houses in a locality. The maximum load demand in the location is in the summer season where the average load demand is 39kWh for the six months of the summer season and the average load demand for the winter season is 15.6kWh. Based on the location of Pakistan the design system of the Renewable Energy System is a hybrid one with an addition of solar PV and will be Grid-connected (Baloch *et al.*, 2019). The rating of the wind generator is such that 75% of the total load demand is divided into a 50% share, between the solar PV and the Wind Energy system. Since the design is made for the summer season and the maximum average load in the month of summer is calculated from Table 1, as 39kWh×0.75×0.5=14.625 kWh per day. The load in kW is calculated as 14.625/24= 0.61 kW and for the 100 homes, the total load calculated demand is 0.61×100=61 kW.

The power factor is roughly taken as unity; since the power converters will nullify all the reactive power as all the power transformer is an active power in "Watts" so the generator power in kVA same as 61 kVA.

Table 1: *Load calculation.*

Months	Total load per day (Wh)	Actual Load (Wh) per day for the wind energy	Days	Total Load in one year (Wh)
Jan	15600	5850	31	181350
Feb	15600	5850	28	163800
Mar	15600	5850	31	181350
Apr	39000	14625	30	438750
May	39000	14625	31	453375
Jun	39000	14625	30	438750
Jul	39000	14625	31	453375
Aug	39000	14625	31	453375
Sep	39000	14625	30	438750
Oct	15600	5850	31	181350
Nov	15600	5850	30	175500
Dec	15600	5850	31	181350
Average	327600	122850	365	3741075

Tradeoff between different topologies on the type of generators

In the case of grid-associated short circuit faults, the SCIG is more superior to DFIG due to its detachability option from the grid. In DFIG 30% of the output power passes via a power converter making it advantageous as low-cost power converters can also be used (Beainy *et al.*, 2016). In the case of altogether effectiveness, robustness, and longevity the direct-drive PMSG system is more superior on offshore sites (Beainy *et al.*, 2016). The power specification determined for a load demand of 100 homes is 61kW. Based on the classification of wind turbine technologies, the design of the wind turbine generator will fall in the medium-size category, with a generator type as Permanent Magnet Synchronous Generator (Patil *et al.*, 2013).

Selection of machine topology

In terms of high reliability, low cost, technical maturity a surface-mounted PM generator is considered to be the best choice according to TOPSIS analysis (Gupta and Singh, 2016). A surface-mounted PM generator has a typical configuration where the magnets are affixed at the top surface of the rotor, hence the name 'Surface Mounted Permanent Magnet' (SMPM) machine. In this setup to balance the centrifugal force, the magnets are affixed to the rotor surface. The orientation of magnets is made in the radial direction but least common in the circumferential direction.

The reactance in the quadrature and direct directions are almost the same. Due to simple rotor contour, amongst other configurations, the construction of the rotor core is the easiest in SMPM (Madani *et al.*, 2015). The surface-mounted configuration is shown below. Due to simple rotor geometry, the non-salient surface-mounted permanent magnet topology is selected to lessen the overall cost of the machine (Madani *et al.*, 2015). In the non-salient machine, the quadrature axis inductance and direct axis inductance are both equal since the permeability of free air is almost equivalent to the permeability of a permanent magnet.

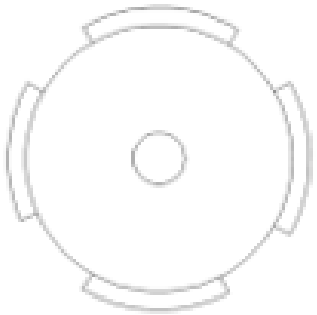

Figure 1: *A Surface mounted rotor for a PMSG.*

Windings

The windings generally use are Distributed Winding, Concentrated Winding, Fractional Slot Winding, and Single Layer Concentrated Non-Overlapping Winding. In terms of efficiency for low-speed applications such as wind turbines, concentrated windings are more efficient to be used (Ghoneim *et al.*, 2016). A Surface mounted rotor for a PMSG and Matlab Simulink design of PMSG are shown in Figure 1 and 3, respectively.

Materials and Methods

Design of a selected machine

The design flow chart is shown in Figure 2.

The following constants like the winding factor K_w, tooth flux density B_t, remnant flux density B_r, Stator flux density B_s and lamination filling factor K_{fill} is taken from the literature review (Hebala *et al.*, 2017; Ghoneim *et al.*, 2016). The methodology of the designed machine has been incorporated in the flow chart. The design of the generator has been evaluated in excel also given in the appendix section. The novelty of the design is based on modifying the slot depth and its dimensions until a difference in magnitude of the area of slot calculated through iteration and area of slot evaluated by equation A_{cs} / K_{fill} reaches the minimum value of 5 % of A_s (area of slot). Consequently, the magnet thickness, stator inner/outer radii, rotor inner/outer radii, air-gap length, and Stack length all change with the modifications based on the size of the PMSG wind turbine generator.

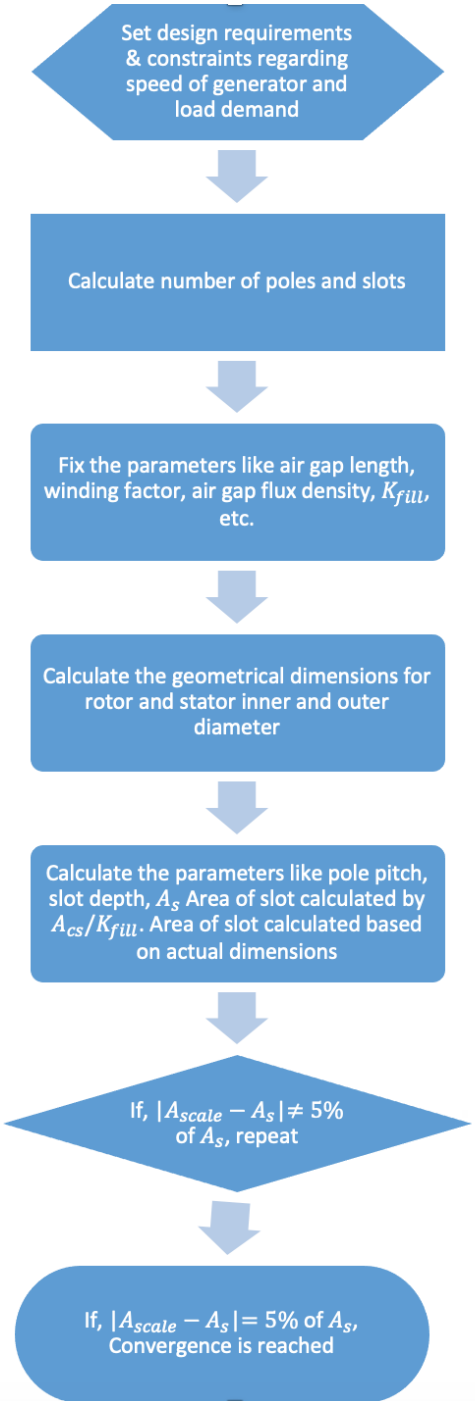

Figure 2: *Design flow chart.*

Results and Discussion

The Matlab Simulink diagram is made after setting the speed at a rated value of 100 rpm, (Madani

et al., 2015). A Low pass (LC) filter is added after rectification to remove higher harmonics while smoothing the curve. The values of inductance and capacitance are set to the values of $50\times10^{-6}H$ and $50\times10^{-6}F$ respectively. The input torque defined by the step input to the PMSG block is readjusted with a step time given at 0.2 while limiting the simulation to a 1-time unit. Average load demand per day calculation for a building apartment for winter and summer seasons as shown in Supplementary Table 2.

The input torque to the generator is calculated as:

$$\text{Torque} = \frac{Calculated\ load, Pm}{Angulare\ Speed\ of\ Rotor\ in\ Rad/Sec} = \frac{60{,}000}{(2\pi/60)\times 100} = 5729.74\ \text{Nm}$$

Resistance of stator, Armature Inductance, Flux linkage, and pair of poles are found to be:
The Resistance of the stator R_s, is calculated as;

$$R_s = \frac{\rho L}{A} \quad \ldots(1)$$

Where ρ is the resistivity of the copper (1.77×10^{-8}), L is the Stack length and A is the area of the conductor, using Equation 1, putting the values calculated in the excel sheet from Supplementary Table 1:

$$R_s = \frac{1.77\text{x}10^{-8}\times Stack\ lenght\ \times N_{ph}}{\frac{\pi Dc^2}{4}}$$

$$R_s = \frac{1.77\text{x}10^{-8}\times 1.095\ \times\ 60}{\frac{\pi 0.0044^2}{4}}$$

$$R_s = 0.3\ \Omega/\text{phase}\ (2)$$

With the addition of 1.92 Ω resistance of the connector and 1.92 Ω resistance of the junction the total resistance of the stator becomes:

$$R_s = 0.31 + 1.92 + 1.92$$

$$R_s = 4.15\ \Omega$$

The stack length L, Coil turns N_{ph} and the diameter of the conductor D_c are taken from Supplementary Table 1).

Armature Inductance is fixed at $H=2X10^{-6}$ *Henry.*

The flux linkage is calculated as;

$$Flux\ Linkage = N_{ph}\times\varphi \quad \ldots(3)$$

Where; flux per pole,

$$\varphi = B_g \times Area\ of\ one\ pole$$ And,

$$Area\ of\ one\ pole = \tau_p \times L_{stack}$$

τ_p, is the pole pitch and B_g is the air gap flux density,

Therefore, using Equation 3,

$$Flux\ Linkage = N_{ph}\times B_g \times \tau_p \times L_{stack}$$

$$= (60\times 0.65\times 38.039\times 1094.81)/(1000\times 1000)$$

$$Flux\ Linkage,\ \Psi = 1.624\ Weber\text{-}turn$$

(values are taken from the Supplementary Table 1).

The number of poles calculated is:

$$P = \frac{120\times f(Hz)}{N(rpm)} \quad \ldots(4)$$

$$\text{P} = \frac{120\times 50}{100}$$

P=60 *poles*

The number of slots N_s is calculated as:

Since the number of slots per pole per phase q=1.

Therefore,

$$N_s = 3\times Poles$$

$$N_s = 3\times 60 = 180\ slots$$

The input parameters for the permanent magnet synchronous generator are given below:

Resistance of the Stator Rs= 4.15Ω
Armature Inductance (H)=2×10⁻⁶ henry
Flux linkage=1.624 Weber-turn
Pair of poles = 30

Sensitivity of the designed machine
The Sensitivity of the designed machine about the flux linkage Ψ, the stator resistance R_s and the armature inductance H are considered. Figure 4, shows the Voltage measurement between terminals A and B, which is about 400 Volts according to the PMSG parameters given in Table 5. It also shows the speed of the rotor which is according to the rated speed of 100 *rpm.*

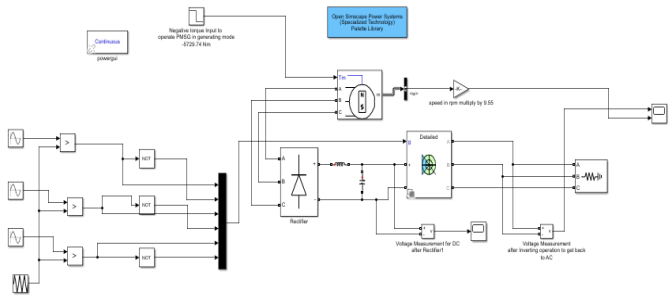

Figure 3: *Matlab Simulink design of PMSG.*

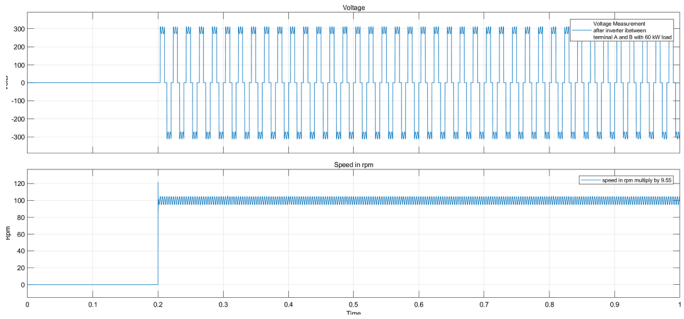

Figure 4: *Voltage Measurement between terminal A and B and Speed in rpm.*

Table 2: *Comparison of different types of generators (Gupta and Singh, 2016).*

Generator type	Energy yield	Cost	Reliability	Grid Supportability	Technical Maturity
SCIG	Least	Least	Highest	Least	Highest
WRIG	Average highest	Highest		Highest	Highest
DFIG	Average highest	Average	Average	Average	Highest
PMSG	Highest	Average highest	Average highest	Highest	Average highest

Table 3: *Constant parameters (Madani et al., 2015).*

Parameter names	Values in units
Winding factor, K_w	0.866
Tooth flux density, B_t	1.8 T
Remnant flux density, B_r	1.6 T
Stator flux density, B_s	1.6 T
Lamination filling factor, K_{fill}	0.45
Electric loading AC	25000*watt-hours*

Variation of flux linkage and its effect on the output load voltage and speed while keeping other parameters constant

By increasing the flux linkage from, a calculated value of 1.624 weber turns to 2.124 weber turns the voltage between terminal voltage and speed of the rotor decreases. It further decreases when the flux linkage is 2.624-weber turns. By decreasing the flux linkage from a nominal value of 0.624 weber-turns the speed of the rotor increases drastically while the voltage across the load between terminal A and B also increases. Constant and designed parameters of PMSG are shown in Table 3 and Table 4.

Table 4: *Parameters of PMSG to be designed.*

Parameters	Value
Pole number	60
Slot number	180
Number of phases	3
Rated speed in rpm	100
Rated output power (W)	60kW
Rated Torque (N.m)	5729.75 Nm
Induced Voltage (V)	230
Estimated efficiency (%)	90%
Winding turns per slot (turns)	5
Stator radius: inner/outer (m) R_{si}, R_{so}	0.729/ 0.762
Rotor radius: inner/outer (m) R_{ri}, R_{ro}	0.696/ 0.726
Air-gap length (m) l_g	0.0015
Magnet thickness (m) l_m	0.001
Stack length (m)	1.094
Slot Depth (m)	0.011
Slot opening Width (m)	0.00254
Tooth width t_w (m)	0.00517
Core material/ Permanent magnet	N30AHNdFeB

Parameters validated through Motor-solve software.

Table 5: *PMSG parameters.*

Name of the Parameter	Calculated value
Flux Linkage Ψ	1.624 weber-turns
Stator Resistance R_s	4.15 ohms
Armature Inductance (H)	2× 10^{-6} H

For flux linkage 2.124 weber-turns

Figure 5, shows voltage between terminal A and B when the flux linkage is increased to 2.124 weber-turns. As we can see the voltage between the two terminals has decreased from the nominal value. It shows the speed of the rotor in rpm which is reduced to 60 rpm.

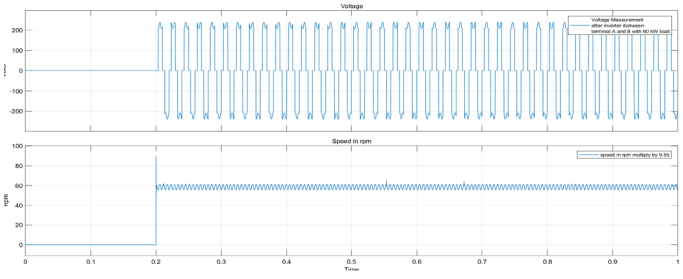

Figure 5: *Voltage Measurement between terminal A and B and Speed in rpm.*

For flux linkage 2.624 weber-turns

Figure 6, shows the voltage between terminal A and B when flux linkage is further increased to 2.624 weber-turns, while the speed of the rotor in rpm when the flux linkage is increased to 2.624 weber-turns.

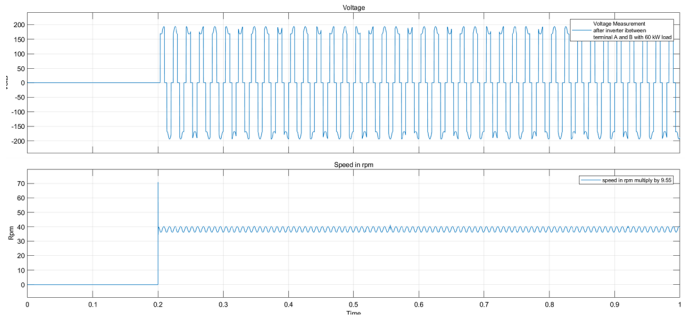

Figure 6: *Voltage Measurement between terminal A and B and Speed in rpm.*

For flux linkage 0.624 weber-turns

Figure 7, shows the voltage across the terminal A and B when flux linkage is reduced to 0.624 weber-turns while showing the speed of the rotor in rpm when the flux linkage is reduced to 0.624 weber-turns. The speed of the rotor has greatly increased to around 680 rpm.

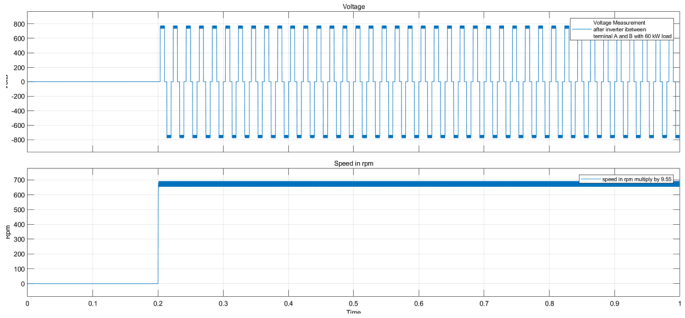

Figure 7: *Voltage Measurement between terminal A and B and Speed in rpm.*

Variation in stator resistance while keeping other parameters constant

On increasing the stator resistance from the calculated value of 4.15 ohms to 4.65 and 5.14 ohms, the voltage between terminal A and B does not change much while the rotor speed in rpm slightly increases. On decreasing the stator resistance to 3.65 ohms, the rotor speed reduces from 100 rpm, while the voltage across the terminals remains unchanged.

For Stator Resistance of 4.65 ohms

Figure 8, shows the voltage between terminal A and B when the stator resistance is increased to 4.65 ohms, while it shows the speed of the rotor in rpm which shows an increment from the rated value.

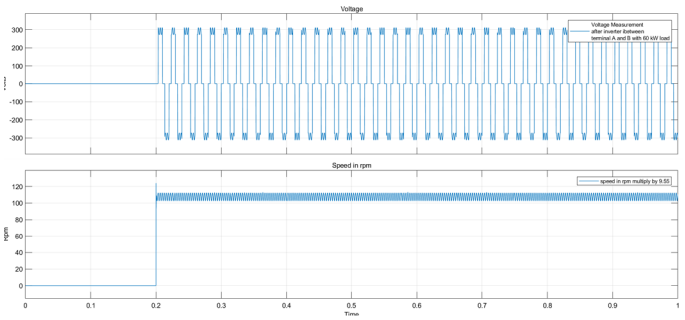

Figure 8: *Voltage Measurement between terminal A and B and Speed in rpm.*

For stator resistance of 3.65 ohms

Figure 9, shows the voltage across the terminal A and B when the stator resistance is reduced to 3.65 ohms, while showing the rotor speed in rpm when the stator resistance is reduced to 3.65 ohms. It shows that speed in rpm to be slightly reduced by 90 rpm.

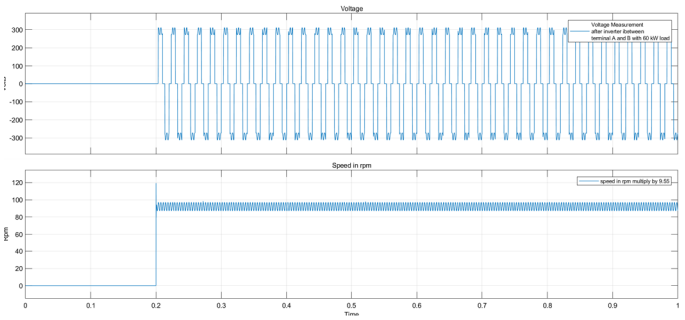

Figure 9: *Voltage Measurement between terminal A and B and Speed in rpm.*

For stator resistance of 5.15 ohms

Figure 10, shows the voltage across the terminal when the stator resistance is increased to 5.15 ohms, while it shows the speed in rpm when the stator resistance is set to 5.15 ohms. It shows that the speed is increased to 118 rpm.

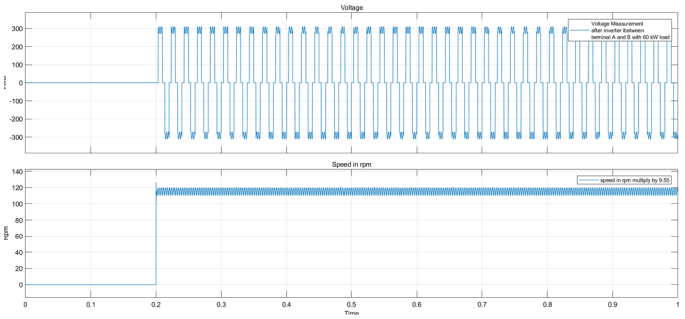

Figure 10: *Voltage Measurement between terminal A and B and Speed in rpm.*

Variation of armature inductance while keeping other parameters constant

On increasing the armature inductance from the

calculated value of $2\times10^{-6}H$ to $2\times10^{-5}H$ and $2\times10^{-4}H$ the voltage across the terminal does not change much while the rotor speed shows an abrupt increase at the step input of 0.2 and we can see disturbances along the line of 100 rpm. By decreasing the value from $2\times10^{-6}H$ to $2\times10^{-7}H$ and $2\times10^{-8}H$ the voltage across the terminal A and B rotor speed remains the same.

For armature inductance of 2xexp-7 henry

Figure 11, shows the voltage across the terminal when the armature inductance is set at $2\times10^{-7}H$, while it shows the speed in rpm when the armature inductance is reduced to $2\times10^{-7}H$.

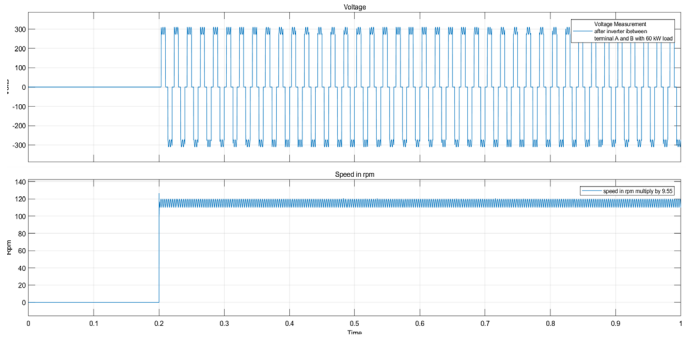

Figure 11: *Voltage Measurement between terminal A and B and Speed in rpm.*

For armature inductance of 2xexp-8 henry

Figure 12, shows the voltage between terminal A and B when the armature inductance is further reduced to $2\times10^{-8}H$, while it shows the speed in rpm when the armature inductance is set to $2\times10^{-8}H$.

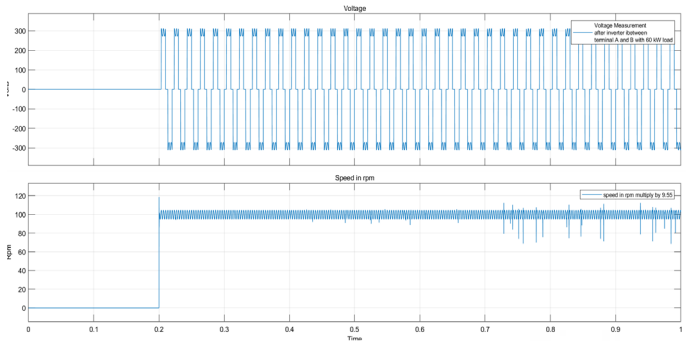

Figure 12: *Voltage Measurement between terminal A and B and Speed in rpm.*

For armature inductance of 2xexp-5 henry

Figure 13, shows the voltage across the terminal A and B when the armature inductance is increased to $2\times10^{-5}H$, while it shows the speed in rpm when the armature inductance is increased to $2\times10^{-5}H$ from the nominal value. We can see a spike in rotor speed at step input of 0.2.

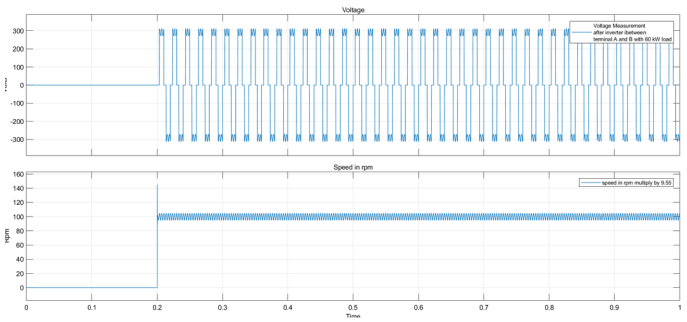

Figure 13: *Voltage between terminal A and B.*

For armature inductance of 2xexp-4 henry

Figure 14, shows the voltage across the terminal A and B when the armature inductance is further increased to $2\times10^{-4}H$, while it shows the rotor speed in rpm when the armature inductance is increased to $2\times10^{-4}H$.

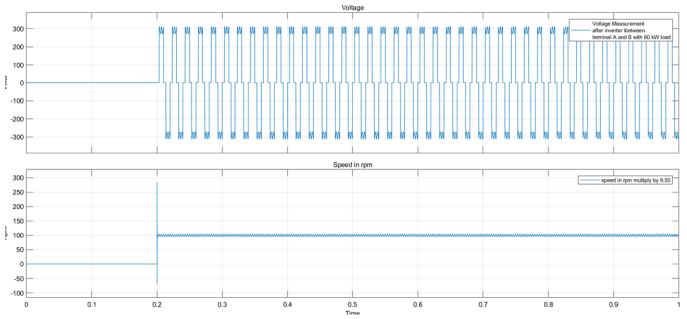

Figure 14: *Voltage between terminal A and B.*

Conclusions and Recommendations

In low-income countries, harvesting energy from wind and solar is considered the most viable option to meet residential demand for a particular locality. However, the designed capacity of the generator could change with the increasing energy demand in different areas. Decentralizing the energy mix into smaller units is an option to lessen the burden on the national grid which will have an impact on reducing the usage of fossil fuels and minimize CO_2 emissions. This paper brings an idea to the town planners and local developers of the power market that electricity can be fed to the residential communities from wind and solar while solving the two renewables' intermittency issues and giving better life quality for the community of that area.

Novelty Statement

The novelty of the design is based on modifying the slot dimensions until a difference in magnitude of area of slot calculated through iteration and area of

slot evaluated by equation A_cs/K_fill reaches the minimum value of 5 % of A_s (area of slot).

Author's Contribution

Shoaib Khan: Writing original draft
Sida Hussain: Rating/specification of wind generators.
Amir Naveed: Research methodology and guidance about wind energy
Nazia Wali: Reviewed and editing technically.
Zafar Ullah: Cross checked the results with published research data
Muhammad Arif: Project administration and Supervision
Muhammad Sadiq: Review of draft
Muhammad Asif: Review on analyz-ing simulation techniques.

Supplementary Material

There is supplementary material associated with this article. Access the material online at:

Conflict of interest
The authors have declared no conflict of interest.

References

Alrikabi, N.K.M.A., 2014. Renewable energy types. J. Clean Energy Technol., 2(1): 61-64. https://doi.org/10.7763/JOCET.2014.V2.92

Baloch, M.H., S.T. Chauhdary, D. Ishak, G.S. Kaloi, M.H. Nadeem, W.A. Wattoo, T. Younas and H.T. Hamid. 2019. Hybrid energy sources status of Pakistan: An optimal technical proposal to solve the power crises issues. Energy Strategy Rev., 24: 132-153. https://doi.org/10.1016/j.esr.2019.02.001

Beainy, A., C. Maatouk, N. Moubayed and F. Kaddah. 2016. Comparison of different types of generators for wind energy conversion system topologies. In: 2016 3rd International Conference on Renewable Energies for Developing Countries (REDEC). IEEE. pp. 1-6. https://doi.org/10.1109/REDEC.2016.7577535

Chiari, L. and A. Zecca. 2011. Constraints of fossil fuels depletion on global warming projections. Energy Policy, 39(9): 5026-5034. https://doi.org/10.1016/j.enpol.2011.06.011

Ghoneim, W.A., A. Hebala and H. Ashour. 2016. A comparative study of winding configuration effect on the performance of low speed PMSG using FEM. In: 2016 18th International Middle East Power Systems Conference (MEPCON). IEEE. pp. 348-352. https://doi.org/10.1109/MEPCON.2016.7836914

Gupta, N. and Y. Singh. 2016. Optimal selection of wind power plant components using technique for order preference by similarity to ideal solution (Topsis). In: 2016 International Conference on Electrical Power and Energy Systems (ICEPES). IEEE. pp. 310-315. https://doi.org/10.1109/ICEPES.2016.7915949

Hebala, A., W.A. Ghoneim and H.A. Ashour. 2017. Different design approaches of surface mounted high performance PMSG. In: 2017 International Conf on Advanced Control Circuits Systems (ACCS) Systems and 2017 Intl Conf on New Paradigms in Electronics and Information Technology (PEIT) IEEE. pp. 85-90. https://doi.org/10.1109/ACCS-PEIT.2017.8303024

Herbert, G.J., S. Iniyan, E. Sreevalsan and S. Rajapandian. 2007. A review of wind energy technologies. Renewable Sustain. Energy Rev., 11(6): 1117-1145. https://doi.org/10.1016/j.rser.2005.08.004

Madani, N., A. Cosic and C. Sadarangani. 2015. A permanent magnet synchronous generator for a small scale vertical axis wind turbine. In: 2015 IEEE International Electric Machines and Drives Conference (IEMDC). IEEE. pp. 48-52. https://doi.org/10.1109/IEMDC.2015.7409035

Patil, N.S. and Y.N. Bhosle. 2013. A review on wind turbine generator topologies. In: 2013 International Conference on Power, Energy and Control (ICPEC). IEEE. pp. 625-629. https://doi.org/10.1109/ICPEC.2013.6527733

Saleem, L. and I. Ulfat. 2019. A multi criteria approach to rank renewable energy technologies for domestic sector electricity demand of Pakistan. Mehran Univ. Res. J. Eng. Technol., 38(2): 443-452. https://doi.org/10.22581/muet1982.1902.18

Shafiee, S. and E. Topal. 2009. When will fossil fuel reserves be diminished? Energy Policy, 37(1): 181-189. https://doi.org/10.1016/j.enpol.2008.08.016